MRS Advances
https://doi.org/10.1557/s43580-024-00941-x

ORIGINAL PAPER

High performance chemiresistive carbon-nanotube ammonia gas sensor surface modified by tantalum oxide (Ta_2O_5) metal nanoparticles

Shah Masheerul Aalam[1] · Mohd Sarvar[1] · Mohd Nadeem Bhat[2] · Monika Tomar[3] · Javid Ali[1]

Received: 25 June 2024 / Accepted: 9 September 2024

Abstract

We have studied the response behaviour of bare and embellished Multiwalled Carbon Nanotubes (MWCNTs) in gas sensing, as well as their gas sensing properties have been thoroughly analysed. Pure tantalum oxide (Ta_2O_5) metal nanoparticles are deposited onto carbon nanotubes using the RF-sputtering technique. In terms of sensing response, the response in a decorated sensor was 565%, much greater than the pristine CNT response of 97%. The entire process was tested with an ammonia gas concentration of 10 ppm at room temperature. We've seen fast response time in pristine MWCNTs (1–15 s) and in embellished MWCNTs it was (1–4 s). The sensitivity value was 50% for pristine, while for the (10 min) decorated MWCNT sensor, it was 79%. According to the observed sensor response graph, a recovery of 75–85% had been achieved. The recovery time of pristine and decorated were seen as (1–14 s) and (1–6 s) respectively.

Introduction

For the past several years, there has been an increased interest in novel materials and treatment techniques for gas sensing applications that can identify gaseous molecules [1]. The goal of gas sensing research is to develop an electronic nose with adequate sensitivity, selectivity, and repeatability to identify every type of gas found in the ambient environment at low concentration levels [2–6]. The most widely utilised of these gases, NH_3 is employed in agriculture, food processing, environmental cleanup, and medical diagnostics. NH_3 gas sensors have been developed based on semiconductor metal oxides such as SnO_2 and ZnO, which need high working temperatures between 300℃ and 400 °C [7, 8]. Because of their various benefits, carbon nanotubes or CNTs show considerable potential in this regard. Many CNT-based gas sensor models, including the gas ionisation sensor, capacitive sensor have been developed in order to use CNTs in NH_3 sensing applications [9–11]. Even if pristine CNTs have the right qualities, there are still certain shortcomings that need to be addressed for them to be used in chemical sensors as effectively as possible. These shortcomings include low sensitivity, poor selectivity, and lengthy recovery times when used at room temperature quicker recuperation.

When using high operating temperatures (between 100 °C and 200 °C), sensors stability can be attained [12]. Because of its low power requirements, room temperature functioning, sensitivity to a wide range of chemicals, and exceptionally low detection threshold, CNT chemical resistance sensors are frequently employed. Since carbon nanotubes have strong conductivity and internal gas detection capabilities, they have been employed as sensors for chemical resistor-based sensors. The benefit of this is that it can build a tiny sensor system [13]. A literature review states that CNTs are commonly decorated with gold, silver, copper, and other metals to boost their sensitivity. This makes it possible to significantly enhance low-temperature functioning, response/recovery qualities, and sensitivity [14]. A survey of the literature indicates that the decoration of Cu and other metal transition particles can greatly enhance the CNT sensor responsiveness. The nanoscale size is necessary to produce adsorption sites for target gas molecules and maximise the amount of electron transport in the CNTs through charge transfer [15].

✉ Javid Ali
javi_reslab@rediffmail.com; jali1@jmi.ac.in

[1] Department of Physics, Jamia Millia Islamia, New Delhi 110025, India

[2] National Institute of Technology, Srinagar (J&K) 190001, India

[3] Miranda House, University of Delhi, Delhi 110007, India

Published online: 19 September 2024

This study describes the synthesis of Multiwalled Carbon Nanotube (MWCNTs) films on a silicon substrate by means of the low pressure chemical vapour deposition (LPCVD) technique, wherein iron (Fe) was employed as a catalyst [15]. Sonication of the silicon (Si) substrate in acetone at 60 °C was the purification process. With the use of field emission scanning electron microscopy (FESEM), the dimensions and composition of the MWCNTs were examined. At room temperature, the NH_3 sensitivity of the MWCNT films was examined using a Kethley 6514 static source meter measuring device. The MWCNTs were coated with a Ta_2O_5-nanoparticle acts as catalyst to improve CNT based sensors response and encourage NH_3 gas contact.

Experimental details

The right-sized N-type (100) silicon substrates were employed. The substrates were ultrasonically cleaned for half an hour with acetone, and then left to air dry. The ready Si substrates were put into the RF-Sputtering chamber, and an iron (Fe) target with a purity of 99.999% was employed to coat the substrates with iron nanoparticles in order to deposit the Fe catalyst precisely. The substrate-target distance was around 8 cm. An often used use of this technique (RF-Sputtering) is surface functionalization. In the RF Sputtering chamber, the necessary vacuum was produced for the high-quality deposition of Fe catalyst. High grade nitrogen (N_2) plasma was created by passing the N_2 gas through the chamber under 50 sccm at a power of 100W and a deposition pressure of 10^{-3}.

Using the LPCVD technique, MWCNTs were produced at 750̊ C under the right, regulated, and optimised conditions. Especially for the production of highly aligned, very pure, and highly dense CNTs. The Fe-deposited substrates were inserted into the LPCVD chamber, and it was then properly closed. The system's rotational pump produced an excellent vacuum within the chamber that was on the order of 10^{-3} Torr. Once the pre-treatment was completed, the temperature was raised to 750 °C. The horizontally aligned quartz tube with the heater chamber, was used to inject the carbon source C_2H_2 30 sccm gas flow at the temperature of 750 °C. Hydrogen (H_2) of 70 sccm and ammonia NH_3 of 30 sccm were both employed as gases. Hydrogen performs the function of the carrier gas, while NH_3 performs the function of the diluting agent.

Tantalum (Ta) coating was accomplished by RF sputtering after the entire process of LPCVD was finished. Ta nanoparticles were decorated on the carbon nanotube sensor synthesised by LPCVD on the Si substrate, which had previously been pre-coated with the iron catalyst. Although during the sputtering process, the 99.99% finest form of tantalum metal serves as the target. Sputtering was carried out every ten minutes. Throughout the procedure, 140 W sputtering power has been given for sputtering the nanoparticles. Throughout the process, the working and starting pressures were 10^{-3} Torr. Following that, the sensor was heated in the presence of oxygen at a temperature of 1000 °C for 9 h to generate an oxide on its surface.

Results and discussion

Initially, the shape and content of the hybrid gas-sensitive nanomaterial were examined using FESEM, EDX, and Raman Spectroscopy. Several methods were employed to examine the resultant nanomaterials.

Field emission scanning *electron* microscope (FESEM)

FESEM from ZEISS Gemini SEM 500, which is used to obtain the samples' surface morphology at a very high resolution. Figure 1A, B below displays the FESEM micrographs of the samples as they were produced. As shown in the picture, the Ta_2O_5 nanoparticles linked to the MWCNTs are indicated by the cluster of brilliant, bright dots. As the deposition rises over time, the density of the spot cluster increases in the spectra (B). The cluster density demonstrates the Ta_2O_5 nanoparticle adhesion on the MWCNT surface. It was calculated that the typical diameter of CNTs was between 40 and 50 nm. As the deposition period increases, the decorated CNT's average diameter rises.

The distribution of the concentration of the carbon and metal decorating nanoparticles is depicted in the figure's (C) and (D) elemental maps of EDX. As seen in Fig. 1 below, the carbon concentration in spectrum C is greater than the carbon concentration in micrograph D. The produced sample MWCNT-Ta_2O_3 nanocomposite's EDX spectrum indicates the existence of carbon concentration and the deposition of metal concentration, as indicated by the micrographs (C) and (D) as seen in Fig. 1 below.

Raman spectroscopy

Utilising Raman (Renishaw) spectroscopy, CNT quality is evaluated. Renishaw's 532 nm excitation laser beam was used to study the CNTs with iron catalysts while they were growing. The G-band, also known as the high energy band in our study, arises at 1563 cm^{-1} in pristine sample and represents the stretching mode of the graphite plane, which covers the dimensions of 1500–1600 cm^{-1}. With a wavelength ranging from 1300 to 1400 cm^{-1}, the D-band is created via defect-induced double resonant Ta_2O_5 virgin, Raman scattering with D-band occurs at 1343 cm^{-1}. With a wavelength range of 2500–2800 cm^{-1}, the G′-band, also known as the

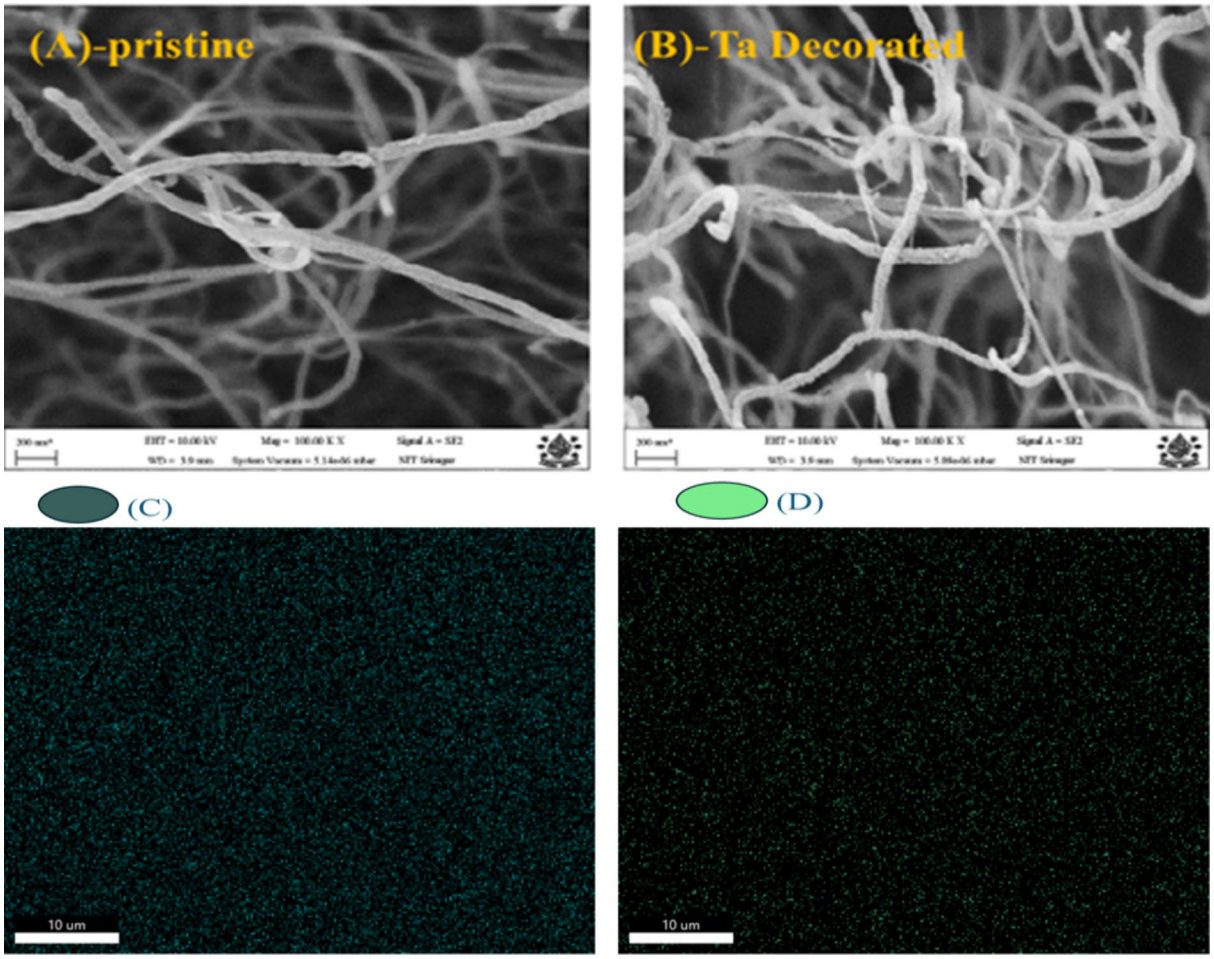

Fig. 1 FESEM micrographs of (**A**) pristine and (**B**) tantalum oxide (Ta_2O_5) decorated and EDX elemental maps (**C**) pristine and (**D**) Ta decorated

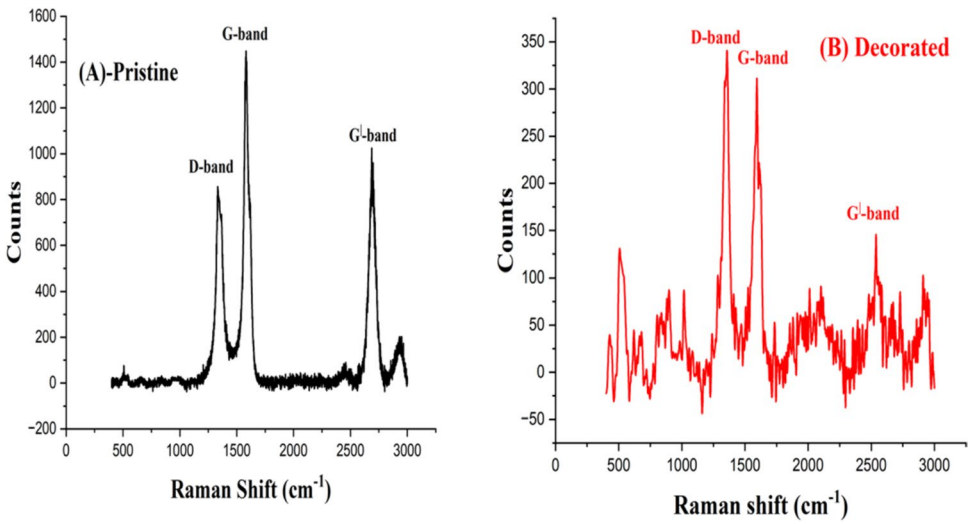

Fig. 2 Raman spectra of the as grown samples (**A**) pristine and (**B**) Ta_2O_5 decorated (10 min) MWCNT sensor

2D band, is a second-order two-phonon process that strongly depends on the energy of the excitation laser (Fig. 2).

Gas sensing studies

The same NH_3 experiments were performed on the MWCNT sensor covered with Ta_2O_5 nanoparticles. Compared to pristine 97% responsiveness in 1–12 s, there was a tremendous enhancement in sensor response magnitude of about 567% in 1–6 s. Once the target gas attained saturation, it was removed from the chamber. High quality, quick response, and complete recovery were seen in decorated sensor when contrasted with the response and recovery characteristics of a pristine MWCNT sensor. This clearly shows that the Ta_2O_5 nanoparticles create areas on the MWCNT surface where gas molecules may interact, which results in the enhanced reaction that is seen in Fig. 3 below A nearly 1.5-fold increase in responsiveness was seen when compared to a plain MWCNT sensor.

However, the pristine MWCNT sensor recorded a higher resistance change in Kilo-ohms, but the Ta_2O_5 -decorated MWCNT sensor revealed a larger resistance shift in Mega-ohms; this difference is seen in Fig. 3 below. When the temperature is too low, the adsorption barrier is not broken down by enough energy to allow target gases to be adsorbed on the sensor's surface. Additionally, because the desorption rate will be higher than the adsorption rate at high operation temperatures, the response will be lower. At the optimal sensing temperature, the adsorption rate and desorption rate are equivalent, and the target gas molecules possess sufficient energy to overcome the adsorption barrier, leading to a strong reaction.

Meanwhile, the sensitivity of the sensor may rise as a result of the metal-CNT interaction. There is a depletion region on the CNT sidewall where Ta_2O_5 nanoparticles are deposited. Because the NH_3 molecules donate electrons to the CNT sidewall, widening the depletion zone and preventing carrier (hole) transit on the CNT wall, the device's conductivity is decreased. The sensor resistance is therefore increased as a result. Since the CNT sensor reacts to NH_3 at room temperature, it becomes immediately sensitive to the gas when it is adsorbed on the CNT film. This is followed by the reaction approaching a saturated value at a certain gas concentration.

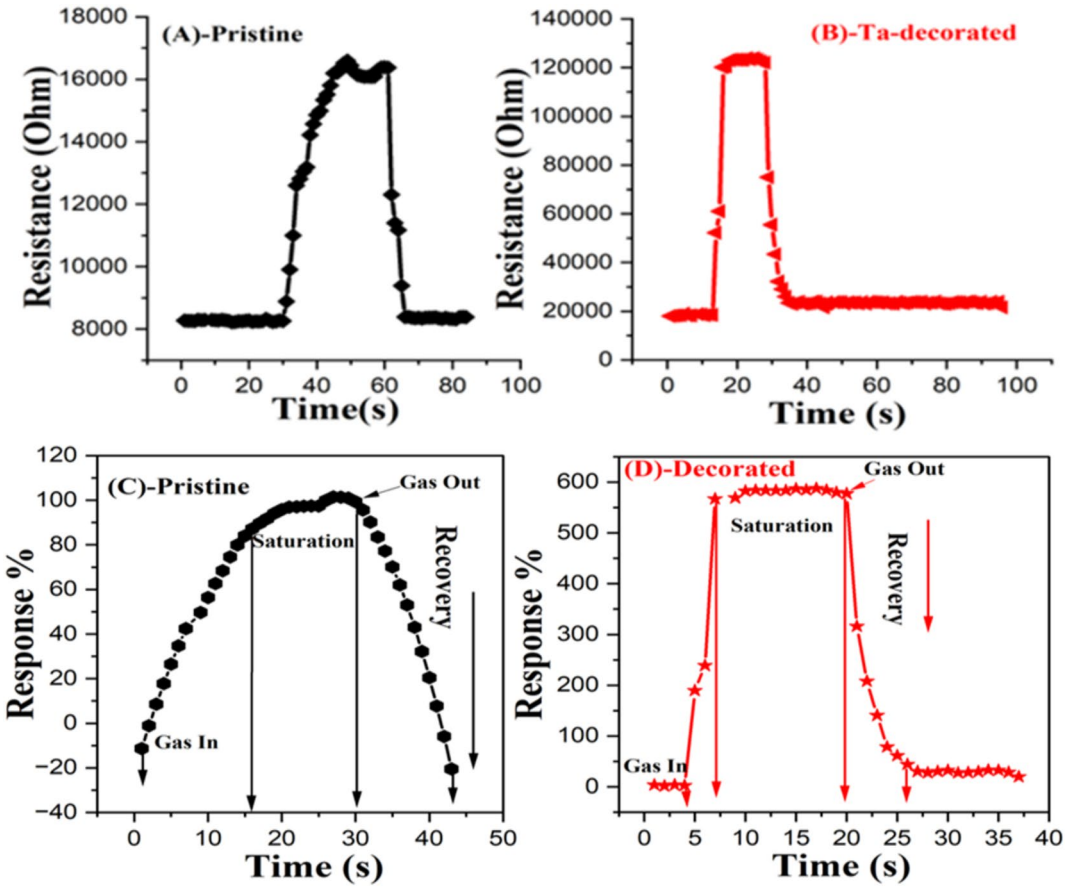

Fig. 3 Resistance variation plots (**A**) pristine (**B**) Ta_2O_5 decorated, and Response plots (**C**) pristine (**D**) Ta_2O_5 decorated MWCNT sensors respectively

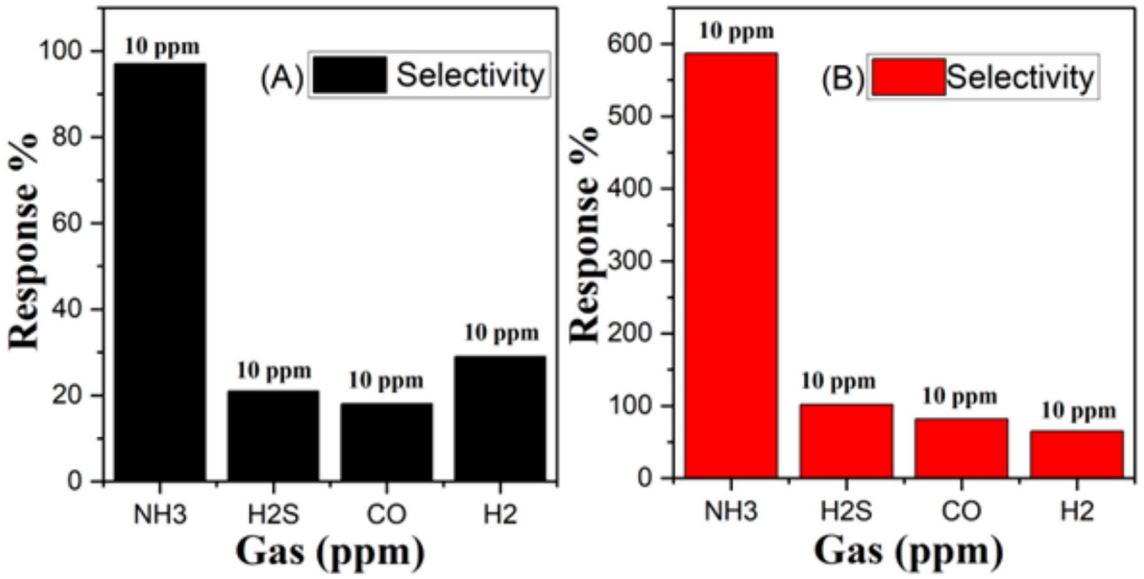

Fig. 4 Measurements of the selectivity of (**A**) Pristine and (**B**) Ta_2O_5 decorated MWCNT sensors

The following formula was used to determine the size of the sensor response:

$$\left[\left(R_{gas} - R_{air}\right)/R_{air}\right] \times 100$$

where R_{gas} and R_{air} stands for the resistance in presence and in absence of the testing/analyte gas respectively.

Using R_a/R_g for the reducing gases and R_g/R_a for the oxidising gases, the sensitivity of the sensors was assessed. The as-prepared samples have a sensitivity of 50% and 79%, respectively. The response curves in Fig. 3. display the obtained responses from the sensing layer. The as-fabricated, flawless MWCNT sensor produced a high-quality sensor response of approximately 97% in pristine, 565% in 10 min decorated, was observed. In Fig. 3A and B depicts the resistance curves of the samples and (C) and (D) depicts the responsive behaviour of the CNT based ammonia gas sensors.

Selectivity of the sensors

Figure 4 illustrates that, in pristine state, less than 50% of the sensor response was seen, but over 97% of the sensor response was recorded for NH_3.The gas selectivity of the MWCNT and MWCNT/Ta_2O_5 sensors at 10 ppm for both as-prepared gas sensors is shown in the bar diagram in Fig. 4. below. In the necessary condition, the immaculate sensor's sensitivity to NH_3 is 50%. Furthermore, among the four gases, the 10 min decorated sensor has the lowest reaction time and highest sensitivity (79% sensitivity to NH_3).

Conclusions

In this study, the sensor demonstrated NH_3 gas responsiveness at values ranging from a few around 10–50 ppm. In addition, Ta_2O_5 nanoparticles were applied to the CNT sidewall to improve the sensors selectivity, sensitivity, and responsiveness. Rapid reaction/recovery time of (1–15sec)/(1–14sec) for unadorned MWCNT and (1–4sec)/(1–6sec) for embellished MWCNT were observed. In percentage terms, the bare sensor's sensitivity is 50%, whereas the embellished sensor's sensitivity is 79%. The 10 minute embellished sample had a response of 565%, which is much better than the pristine response of 97%. After the target gas is injected into the chamber, there is a noticeable rise in the sensor's resistance. A good response, resistance variation, sensitivity was seen in the as prepared sensors.

Acknowledgments We are all appreciative of the characterisation techniques provided by the Centre for Research Facility (CRF) National Institute of Technology, Srinagar, including FESEM, Raman, and EDX. We also appreciate that the University of Delhi (Miranda House) provided us with the sensing apparatus. Additionally, I (S M Aalam) am thankful to the Indian government's Ministry of Higher Education for awarding me the Prime Ministers Research Fellowship (PMRF) under the PMRF-ID, 3302523 under lateral entry scheme in the May cycle of 2022.

Author contributions Shah Masheerul Aalam: Conceptualization, Methodology, Data curation, Formal analysis, Writing the original draft, Writing—review & editing. Mohd Sarvar: Visualization, Validation, Methodology. Mohd Nadeem Bhat: Validation, Visualization. Monika Tomar: Visualization. Javid Ali: Conceptualization, Supervision, Resources, Writing—review & editing.

Funding The authors state that there are no known financial conflicts of interest or intimate personal ties that may have influenced the findings of the research.

Data availability The completed report contains all the data generated or examined during this investigation.

Declarations

Competing interest There are no disclosed conflicts of interest for the authors.

References

1. S. Sharma, M. Madou, Philosophical transactions of the royal society a: mathematical. Phys. Eng. Sci. **370**(1967), 2448–2473 (2012)
2. S. Deshmukh, R. Bandyopadhyay, N. Bhattacharyya, R.A. Pandey, A. Jana, Talanta **144**, 329–340 (2015)
3. F. Röck, N. Barsan, U. Weimar, Chem. Rev. **108**(2), 705–725 (2008)
4. M.M. Raza, S.M. Aalam, M. Sadiq, M. Sarvar, M. Zulfequar, S. Husain, J. Ali, J. Mater. Sci.: Mater. Electron. **33**(3), 1211–1227 (2022)
5. M. Sarvar, M.M. Hasan Raza, S.M. Aalam, M. Sadiq, M.S. Khan, M. Zulfequar, J. Ali, Nano **17**(5), 2250036 (2022)
6. M.M. Raza, S. Khan, S.M. Aalam, M. Sadiq, M. Sarvar, M. Zulfequar, S. Husain, J. Ali, "Carbon Trends" **5**, 100127 (2021)
7. D.G. Sarala et al., Analyt. Chim. Acta **568**, 41–46 (2006)
8. N. Van Hieu, Sens. Actuators B: Chem. **150**(1), 112–119 (2010)
9. J. Huang, J. Wang, Gu. Cuiping, Yu. Kun, F. Meng, J. Liu, Sens. Actuators, A **150**(2), 218–223 (2009)
10. Y. Chen, F. Meng, M. Li, J. Liu, Sens. Actuators, B Chem. **140**(2), 396–401 (2009)
11. G. Zhou, M. Hara, J. Phys. D Appl. Phys. **36**(21), L109–L114 (2003)
12. M.N. Norizan et al., RSC Adv. **10**, 43704–43732 (2020)
13. S.M. Aalam et al., ACS Omega **9**, 4486–4496 (2024)
14. Aalam, Shah Masheerul, Mohammad Moeen Hasan Raza, Mohd Sarvar, Mohd Sadiq, Md Faiz Akram, and Javid Ali. *International Conference on Nanotechnology: Opportunities and Challenges*, pp. 407–413. Singapore: Springer Nature Singapore, 2022.
15. M. Sarvar et al., J. Mater. Sci.: Mater. Electron. **35**, 589 (2024)